Biogeosciences Discuss., https://doi.org/10.5194/bg-2019-69
Manuscript under review for journal Biogeosciences
Discussion started: 4 April 2019

Biogeosciences Discussions Open Access EGU

Nutrient cycling in supraglacial environments of the Dark Zone of the Greenland Ice Sheet

Alexandra T. Holland[1], Christopher J. Williamson[1,2], Fotis Sgouridis[4], Andrew J. Tedstone[1], Jenine McCutcheon[5], Joseph M. Cook[6], Ewa Poniecka[7], Marian L. Yallop[2], Martyn Tranter[1], Alexandre M. Anesio[1,3], and The Black & Bloom Group*

[1]Bristol Glaciology Centre, School of Geographical Sciences, University of Bristol, Bristol, BS8 1HB, UK.

[2]School of Biological Sciences, University of Bristol, 24 Tyndall Avenue, Bristol, BS8 1TQ, UK.

[3]Department of Environmental Science, Aarhus University, Roskilde, 4000, Denmark.

[4]School of Geographical Sciences, University of Bristol, Bristol, BS8 1RL, UK.

[5]School of Earth and Environment, University of Leeds, Leeds, LS2 9JT, UK.

[6] Department of Geography, University of Sheffield, Winter Street, Sheffield, S3 7ND, UK

[7]School of Earth and Ocean Sciences, Cardiff University, Main Building, Park Place, Cardiff, CF10 3AT, UK.

*A full list of authors and their affiliations appears at the end of this paper.

Correspondence to: Alexandra T. Holland (Ah16063@brisol.ac.uk)

Abstract. Glaciers and ice sheets host abundant and dynamic communities of microorganisms on the ice surface (supraglacial environments). Recently, it has been shown that Streptophyte ice algae blooming on the surface ice of the south-west coast of the Greenland Ice Sheet are a significant contributor to the 15-year marked decrease in albedo. Currently little is known about the constraints, such as the nutrient cycling, on this large-scale algal bloom. In this study, we present a preliminary data set that investigates the conversion of dissolved inorganic nutrients to the dissolved organic phase occurring in these darkening surface ice environments. Our results show a clear dominance of the organic phase, with 93% of the total dissolved nitrogen and 67% of the total dissolved phosphorus in the organic phase. Correlations between algal abundance and dissolved organic carbon and nitrogen, indicate ice algae are driving the dissolved nutrient phase shift occurring in these supraglacial environments. Dissolved organic nutrient ratios in these supraglacial environments are notably higher than the Redfield Ratio (DON:DOP= 49, 78, 116) and DOC:DOP= 797, 1166, 2013), suggesting these environments may be phosphorus limited.

Biogeosciences Discuss., https://doi.org/10.5194/bg-2019-69
Manuscript under review for journal Biogeosciences
Discussion started: 4 April 2019

1. Introduction

There has been a significant increase in the net mass loss of the Greenland Ice Sheet (GrIS) during the past two decades (Rignot and Kanagaratnam, 2006;Rignot et al., 2011;Shepherd et al., 2012). The average rate of mass loss increased from 34Gt yr^{-1} to 215Gt yr^{-1} between 1992 and 2011 (Sasgen et al., 2012). Solid ice discharge only accounts for 32% of the total mass loss since 2009, making surface melt the primary driver for the measured increase in ice mass loss (Enderlin et al., 2014). There are two major reasons for this marked increase in surface melting. First, the extent of bare, melting surface ice increased, on average, by 7158 km^2 per year from 2000 to 2014 (Enderlin et al., 2014;Shimada et al., 2016). Second, the albedo of bare surface ice areas declined between 2000 and 2012, with south-west Greenland exhibiting the greatest decrease in albedo of up to 18% (Box et al., 2012). In this region a persistent Dark Zone, some 20-30km inland and ~50 km wide, has reoccurred annually since at least 2001 (Box et al., 2012;Stroeve et al., 2013;Wientjes and Oerlemans, 2010;Tedstone et al., 2017). Shimada et al., (2016) found that there was significant variability in the annual extent of the Dark Zone, which may be the result of both inter-annual climatic variability and factors associated with the ice surface such as melt-out of ancient particles (Tedstone et al., 2017).

Both snow and bare ice albedo are reduced by light absorbing impurities (LAIs), which include biological and mineralogical substances (Gardner and Sharp, 2010). Types of LAI include atmospheric dust and black carbon, cryoconite, and particulates within the meteoric ice that melt out during the ablation season (Wientjes et al., 2012;Cook et al., 2016b;Warren and Wiscombe, 1980, 1985;Gardner and Sharp, 2010;Warren, 1984). The importance of biological LAI, specifically Streptophyte ice algae that form significant algal blooms in surface ice environments during summer ablation seasons, as a factor in albedo decline has been identified in recent years (Yallop et al., 2012). Its effect has become known as "bioalbedo", which is derived from the original term "biological albedo reduction" (Cook et al., 2017a;Kohshima et al., 1993). The bioalbedo effect is attributed to a combination of the heavily pigmented nature of the ice algal cells, including unique dark UV-VIS absorbing pigment, purpurogallin, in the ice algae, which is postulated to provide photo-protection from the extreme solar radiation in supraglacial environments, and the abundance of cells apparent during bloom progression (up to ~10^4 cells ml^{-1} surface ice) (Remias et al., 2012;Williamson et al., 2018). Tedstone et al., (2017) concluded that ice algal blooms are the main factor responsible for inter-annual variability in the extent, magnitude and duration of the Dark Zone and seem to be regulated by climatic drivers including the June-July-August sensible heat flux anomaly and the timing of snow-line retreat. The spatial extent of heavy ice algae blooms may be linked to the availability of particles melting out of the ancient meteoric ice, however the linkage between particles and algae is not presently understood (Tedstone et al., 2017). Furthermore, within the Dark Zone Yallop et al., (2012) noted significant spatial heterogeneity in the ice algal surface ice colonisation, varying on length scales of cm to tens of meters.

Carbon, nitrogen and phosphorus are essential for all living organisms as they provide the basis for cellular mass and all metabolic activity (Redfield et al., 1963). As carbon is usually in ready supply in surface ice environments, nitrogen and phosphorus are more likely the limiting factors for growth and activity of microorganisms (Stibal et al., 2009;Lutz et al., 2017). The presence of such large-scale algal blooms in the Dark Zone, with cell abundances as

high as 8.5 x 10^4 cells ml^{-1}, might suggest that these environments are nutrient-rich (Stibal et al., 2017a). However, the current literature suggests that supraglacial environments are extremely oligotrophic (Stibal et al., 2009;Stibal et al., 2008b;Hawkings et al., 2016;Telling et al., 2011;Telling et al., 2012). A comprehensive review of nitrogen concentrations in Greenland ice was conducted by Wolff (2013), who reported that mean dissolved inorganic nitrogen concentrations in ice cores are 1.4 µmol l^{-1}, with nitrate and ammonium composing 0.97 µmol l^{-1} and 0.45 µmol l^{-1}, respectively. There are relatively few measurements of nutrient concentrations in surface ice environments in the Dark Zone. Values of average nitrate concentrations near the K Transect east of Kangerlussuaq, which passes through the Dark Zone, are 0.6 ± 0.1 µmol l^{-1} for ice located between 17-79km from the ice sheet margin (Telling et al., 2012). Phosphate concentrations are reported as being below the detection limit (Telling et al., 2012). In contrast, dissolved inorganic nitrogen concentrations in snow sampled before the start of the ablation season at the margin of the GrIS were reported as higher than surface ice concentrations, with an average of 1.4 µmol l^{-1} (Telling et al., 2012). We anticipate that this average snow concentration may be an upper limit for the Dark Zone during the height of the ablation season, given the high concentrations of ice algae that occur during blooms.

An efficient balance of nutrient uptake and remineralization occurs in many aquatic environments, specifically those with a planktonic system (Dodds, 1993) allowing nutrient to accumulate in biotic mass over time. Microbial nutrient cycling in polar glacier aquatic environments, such as cryoconite holes, is also extremely active, and as a consequence, dissolved macronutrients tend to concentrate into the dissolved organic phase (Telling et al., 2014;Stibal et al., 2008a;Stibal et al., 2008b). To date, dissolved organic nitrogen and phosphorus concentrations for surface ice environments in the Dark Zone have not been reported, and we contend that this may be an important omission in our understanding of Dark Zone microbial nutrient cycling. Knowledge of both the dissolved inorganic and organic phases of nitrogen, phosphorus and carbon may be crucial to better understand ice-surface nutrient cycles and how ice algae can retain and recycle their limited nutrients to sustain the large-scale blooms observed in this region of the Greenland Ice Sheet.

The aims and objectives of this study, therefore, are threefold. First, we aim to quantify nutrient concentrations in the supraglacial environments of the Dark Zone during the peak ablation season. Second, we determine the relative importance of dissolved inorganic and organic nutrients during the peak ablation season when microbial recycling is likely to have the greatest influence on the dissolved inorganic and organic ratios. Last, we investigate if there are systematic differences in nutrient concentrations in highly colonized surface environments compared to others with lower levels of ice algal biomass.

2. Methods

2.1 Field Site and Sampling

A field camp was established within the Dark Zone, adjacent to Kangerlussuaq, during the summer of 2016. The camp was located approximately 30 km inland from the ice margin, near to the 'S6' weather station on the K-

transect (Fig 1; 67º04'43.3" N, 49º20'29.7" W). Samples were collected from a designated area of approximately 500 x 500 m, which included surface ice, supraglacial stream and cryoconite hole habitats. Sampling occurred at approximately three-day intervals from 15th of July to 14th of August 2016. Given spatial heterogeneity apparent in ice algal distributions, a categorical sampling strategy was employed whereby five main habitats were sampled; surface ice with three differing amounts visible impurities (referred to here as ice with "low", "medium", and "high" visible impurities), supraglacial stream water, and cryoconite hole water (Fig 2) (Yallop et al., 2012). Surface ice habitats were sampled from a 1x1 meter area chosen at random, from which the top ~2 cm of ice was removed using a pre-cleaned ice saw. Samples of surface ice, supraglacial stream water and cryoconite hole water were collected for the analysis of dissolved inorganic and organic nutrients and dissolved organic carbon (DOC). Algal cell abundances were determined on surface ice samples only. Ice collected for nutrient analysis and algal cell abundance was placed into a clean/sterile Whirl-pak™ bag, while that collected for DOC analysis was transferred into a glass jar that was first rinsed three times with sample. Ice samples were left to melt overnight in the lab tent, typically taking 4-5h. Supraglacial stream water samples for nutrient analysis were collected using high-density polyethylene plastic bottles (Nalgene™), whereas those for DOC analysis were collected in glass jars. Both sampling containers were rinsed three times with sample prior to collection. Cryoconite hole water used for nutrient and DOC analysis was collected using a large pipette and transferred into a Nalgene™ bottle or glass jar, respectively. The large pipette and collection vessels were rinsed three times with sample prior to collection.

Ice melt and water samples for nutrient analysis were filtered through a 25 mm, 0.22 µm cellulose nitrate inline syringe filter (Whatman™) and stored in high density polyethylene plastic bottles (Nalgene™; 30mL). The bottles were immediately frozen and stored at a temperature of -20°C, using a Waeco 32L Freezer. Prior to filtration,15 ml of the homogenised ice melt and water samples were subsampled and fixed using 25% glutaraldehyde at 2% final concentration for quantifying algal cell abundance. These fixed samples were stored outside in the dark at ambient ice sheet temperatures. Ice melt and water samples for DOC analysis were filtered using a glass filtration column and a furnaced 47 mm, 0.7 µm GF/F. The filtration column was washed three times with sample water prior to collection of the filtrate. The filtrate was stored in pre-furnaced amber glass vials and acidified with 100 µL of 1M HCL. They were chilled to a temperature of ~3˚C by storing the samples in a box at ambient air temperature. The samples were maintained at this temperature during transport and in storage at the LowTex Laboratory at the University of Bristol. Nutrient samples were thawed immediately prior to analysis using a ~40˚C hot water bath. Procedural blanks (*n=10*) were collected over the course of the sampling season, by processing deionised water in place of sample.

2.2 Analytical Methods

Algal cell abundance was quantified using a Fuchs-Rosenthal haemocytometer (Lancing, UK) on a Leica DM 2000 epifluorescence microscope with attached MC120 HD microscope camera (Leica, Germany). For samples containing sufficient cell abundance, a minimum of 300 cells were counted to ensure adequate assessment of assemblage diversity (Williamson et al., 2018).

TDN (total dissolved nitrogen) is the sum of DIN (dissolved inorganic nitrogen) and DON (dissolved organic nitrogen). DIN species include NH_4^+, NO_2^- and NO_3^-. NH_4^+ was quantified spectrophotometrically using a Lachat QuickChem® 8500 Series 2 Flow Injector Analyzer (FIA; QuickChem® Method 31-115-01-1-I). Measurements were based on a salicylate-hypochlorite alkaline reaction method measured at 660nm (Solorzano, 1969). The limit of detection (LoD) was 0.62 µM. LoD was determined by dividing the standard deviation of the response of the calibration curve by the slope of the calibration curve, then multiplying the result by 3 (Shrivastava and Gupta, 2011). Precision was ±2.1%, and accuracy was +8.5%, as determined from comparison with a gravimetrically diluted 1000 mg L^{-1} NH_4^+-N certified stock standards to a concentration of 1.1 µM. (Sigma TraceCERT®). NO_2^- and TON (NO_2^- + NO_3^-) were quantified spectrophotometrically using a Gallery Plus Automated Photometric Analyzer (Thermo Fisher Scientific, UK). This combination of analysis allows the original NO_3^- concentration to be determined by subtracting NO_2^- from TON. TDN was determined after digesting the samples with potassium persulfate and measuring as TON as above (Grasshoff et al., 1999). DON was then estimated by the difference of the original TON and NH_4^+ from the TDN of the persulfate digestion (DON=TDN- NH_4^+- NO_2^- - NO_3^-). Measurements were based on the hydrazine-sulfanilamide reaction method measured at 540nm. The LoD was 0.14 µM (NO_2^-), 0.64 µM (TON) and 0.87 µM (TDN). Precision was ±0.87% (NO_2^-), ±1.17% (NO_3^-) and ±0.63% (TDN), and accuracy was -4.04% (NO_2^-), -8.07% (NO_3^-) and -5.7% (TDN), as determined from comparison with gravimetrically diluted 1000 mg L^{-1} NO_2^-N and NO_3^-N certified stock standards to a concentration of 0.71 µM (NO_2^-), 1.4 µM (NO_3^-) and 7.1 µM (TDN) (Sigma TraceCERT®).

TDP (total dissolved phosphorus) is the sum of DIP (dissolved inorganic phosphorus, principally PO_4^{3-}) and DOP (dissolved organic phosphorus). The same persulfate digestion method described for TDN was used to measure TDP as PO_4^{3-}. DOP is determined by the subtraction of DIP in the undigested sample from the TDP in the digested sample. PO_4^{3-} in both the undigested and the digested samples was quantified using a Lachat QuickChem® 8500 Series 2 Flow Injector Analyzer (FIA; QuickChem® Method 31-115-01-1-I) using the molybdenum blue method measured at 880nm. The LoD was 0.02 µM (PO_4^{3-} and TDP). Precision was ±1.6% (PO_4^{3-}) and ±3.1% (TDP), and accuracy was +2.3% (PO_4^{3-}) and +5.0% (TDP), as determined from comparison with gravimetrically diluted 1000 mg L^{-1} PO_4-P certified stock standards to a concentration of 0.65 µM (Sigma TraceCERT®). All DIN, DON, DIP and DOP data were water blank-corrected using values from the respective field procedural blanks (Table 1).

DOC concentrations were quantified using a Shimadzu TOC-L Organic Carbon Analyzer, with a high sensitivity catalyst. Non-purgeable organic carbon (NPOC) was measured after acidification of samples with HCL and catalytic combustion (680°C) of dissolved organic carbon to carbon dioxide, which was then measured by infrared absorption. The LoD was 9.5 µM. Precision was ±2.4% and accuracy was -5.9%, as determined from comparison with gravimetrically diluted 1000 mg L^{-1} TOC certified stock standards to a concentration of 83.3 µM (Sigma TraceCERT®).

2.3 Data Analysis

All statistical analysis was performed in RStudio v.1.1.414 (RStudio, Inc 2018). Identification of statistical differences between nutrient, DOC concentrations and algal cell abundance between different habitats was achieved using 1-way analysis of variance (ANOVA) or t-test comparisons, with post-hoc Tukey HSD analysis applied to all significant ANOVA results. Linear regression models and Pearson's product-moment correlations were used to identify correlations between DON, DOC and algal cell abundance. Homogeneity of variance and normality of distribution were tested prior to all parametric analyses, and model assumptions were verified by examination of model criticism plots.

3. Results

3.1 Algal Cell Abundance

Algal cell abundance increased significantly with the amount of visible impurities seen on the ice surface, as shown in Figure 3 ($F_{2,54}$=26.1, p<0.0001). The mean (± standard error) concentrations in the three surface ice habitats were: 99.5 ± 23.9 cells mL^{-1} for ice with low visible impurities, 3850 ± 530 cells mL^{-1} for ice with medium visible impurities and 9800 ± 1570 cells mL^{-1} for ice with a high loading of visible impurities. A significant linear relationship was apparent between algal cell counts and DOC in surface ice habitats (R^2=0.1, p<0.01, n=57). Highly significant Pearson's product-moment correlations were apparent between average algal cell counts and DON and DOC surface ice concentrations (t_3=3.5, p<0.05, r=0.9 and t_3=5.4, p<0.01, r=0.95, respectively).

3.2 Nitrogen

Fifty-four DON samples and 41 DIN samples had concentrations above the respective LoD's. The field blank corrected mean (± standard error) DIN and DON mean concentrations for all five supraglacial environments are displayed in Figure 4. Nearly all the DIN was comprised of NH_4^+, with little to no presence of NO_2^- or NO_3^-. Overall, mean DON concentrations for the surface ice habitats, which range from 0-14.0 µM, are significantly higher ($F_{1,71}$=12.4, p<0.0001) than mean DIN concentrations, which range from 0-1.1 µM (Figure 4). Additionally, DON concentrations increase significantly from low to medium and low to high visible impurity loadings ($F_{4,71}$=19.8, p<0.05, $F_{4,71}$=19.8, p<0.001, respectively). T-tests revealed significant differences between DON and DIN in all supraglacial environments except cryoconite hole water (low: t_{36}=3.6, p<0.001, medium: t_{36}=5.3, p<0.0001, high: t_{36}=7.4, p<0.0001, stream: t_{36}=-2.6, p<0.01).

3.3 Phosphorus

Seventy-four DOP samples and 40 DIP samples had concentrations above the LoD. The field blank corrected mean (± standard error) concentrations for all five supraglacial environments are shown in Figure 5. Half of the DIP

values fell below the LoD. Mean concentrations for the remaining 40 DIP concentrations ranged from 0-0.07 µM. DOP concentrations were at least two times higher than the DIP values, with mean DOP values ranging from 0-0.15 µM. DOP concentrations in cryoconite hole and supraglacial stream water fell below the LoD. DOP concentrations were significantly higher than DIP concentrations in all three surface ice habitats (low: t_{36}=3.1, p<0.01, medium: t_{36}=2.1, p<0.05, high: t_{36}=3.7, p<0.001).

3.4 DOC

Fifty-nine samples had concentrations above the LoD. DOC concentrations increased with the amount of visible impurities present in surface ice habitats, as shown in Figure 6, with a significant difference between ice with high and low visible impurity loading ($F_{4,74}$=6.8, p<0.01). The field blank corrected mean (± standard error) values for DOC were 83.0 ± 23.5 µM, 173 ± 29.9 µM and 242 ± 43.6 µML^{-1} for ice with low, medium and high visible impurities, respectively. The corresponding values for supraglacial stream water and cryoconite hole water were 30.3 ± 13.5 µM and 49.6 ± 33.3 µM, respectively. DOC concentrations in supraglacial stream and cryoconite hole water were significantly lower than ice with high visible impurities ($F_{4,74}$=6.8, p<0.001, in both cases).

4. Discussion

4.1 Dominance of dissolved organic phase over dissolved inorganic phase in ice surface environments.

Dissolved organic nutrients dominate dissolved inorganic nutrients in the surface ice environments of this region of the Dark Zone (Fig 4 and 5). Ninety three percent of the total dissolved nitrogen and ~ 67% of the total dissolved phosphorus found in surface ice habitats was in the dissolved organic phase. To date this organic phase dominance has not been documented in studies of fresh snow or ice cores from the GrIS. As previously mentioned, Telling et al., (2012) reports DIN concentrations in snow found in the margin of the GrIS to be 1.4±0.2 µM L^{-1}, with DON concentrations as non-detectable. Furthermore, the comprehensive review conducted by Wolff (2013) states that mean DIN concentrations in ice cores from Greenland are1.4 µM L^{-1}, while DON concentrations are also non-detectible. This suggests that potential inputs of nutrients to supraglacial environments, such as fresh snow and melting meteoric ice, are strongly dominated by the dissolved inorganic phase. By contrast, the phase association of dissolved nitrogen at the ice surface shifts primarily to the dissolved organic phase during the peak ablation season (July and August). The timing of this shift in nitrogen coincides with the appearance of the annual Dark Zone and ice algal blooms (Tedstone et al., 2017). This is further supported by Williamson et al., (2018) who conducted a transect across the south-west GrIS Dark Zone and documented the extensive and wide-spread algal bloom comprised of pigmented autotrophs during late July and August of 2016. Figure 3 also clearly shows that algal abundance increases in the ice with low, medium and high visible impurities, suggesting that algal cells comprise much of the visible impurities. We therefore hypothesise that the algae present in these blooms drive the shift in nutrients during the peak ablation season from the dissolved inorganic phase to the dissolved organic phase.

4.2 Association of dissolved organic nutrients and algal abundance

Efficient conversion of dissolved inorganic to dissolved organic nutrients by ice algal assemblages is supported by the strong corroboration between average DON and DOC surface ice concentrations and ice algal abundances measured from the same samples. A closer inspection of the data revealed the presence of a high degree of variability. For example, despite the weak linear association apparent in Figure 7, DOC compared to algal cell counts were significant at the 95% level. The variability within these data is likely driven by the highly dynamic nature of the supraglacial environment. For example, the upper ice surface can be characterised as a perched aquifer, with water percolating through the highly permeable surface ice transporting solutes, gases, organic matter and microbial cells both vertically and horizontally (Irvine-Fynn et al., 2012;Christner et al., 2018;Cook et al., 2016c).

We interpret these data to demonstrate that ice algal assemblages are the main producers of the dissolved organic nutrient stocks within the melting surface ice of the GrIS, consistent with previous studies in glacial, freshwater and marine aquatic environments (Musilova et al., 2017;Johannes and Webb, 1970;Lampert, 1978). Ice algae that bloom in these environments rapidly uptake inorganic nutrients, which are derived from a number of possible sources, including the atmosphere, wet and dry deposition, and snow and ice-melt (Kuhn, 2001;Maccario et al., 2015). This results in an increase in the mass of nutrients held in the microbial biomass, and an increase in dissolved organic nutrients as a by-product of the vital intracellular processes and decomposition of the ice algae. An efficient microbial loop, which balances dissolved inorganic nutrient uptake by autotrophic organisms and remineralization by heterotrophic organisms, is often reached in more temperate freshwater aquatic environments (Dodds, 1993). By contrast, work on surface ice near the margin of the GrIS demonstrated bacterial production that was 30 times less than the net primary production of ice algal communities (Yallop et al., 2012). A similar 30:1 ratio was also found by a study conducted in the same study area of the Dark Zone during the 2016 ablation season (Nicholes et al., in review). Dominance of dissolved organic nutrients in surface ice environments highlighted in the present study, in combination with reduced secondary production relative to net primary production in the same environments, indicates reduced capacity of the microbial loop for remineralization of organic nutrient stocks (Nicholes et al., in review; Yallop et al., 2012). This assertion is consistent with the findings of previous studies in polar glacier aquatic environments (Stibal et al., 2009;Stibal et al., 2008a;Stibal et al., 2008b). For example, Stibal et al., (2008) reported that ~70% of the total dissolved nitrogen and ~60% of the total dissolved phosphorus found in supraglacial channel, cryoconite hole and glacier runoff environments of a Svalbard glacier were in the dissolved organic phase. This suggests that conversion of dissolved inorganic to dissolved organic nutrients by autotrophs in melting surface ice environments may be a common process on many glacier surfaces.

4.3 Retention of nutrients at ice sheet surface

The intense solar radiation received by glacier and ice sheet surfaces produces internal melting and density reduction within the near-surface ice, resulting in a unique porous surface ice layer also known as the weathering crust (Müller and Keeler, 1969;LaChapelle, 1959;Munro, 1990). The porous nature of the weathering crust allows flow paths to

form through the water table that exists within the surface ice (Christner et al., 2018;Irvine-Fynn et al., 2012;Rassner et al., 2016;Cook et al., 2016c). These flow paths serve as important links between different supraglacial environments and are believed to transport microbes and nutrients via subsurface flow (Irvine-Fynn et al., 2012;Hoffman et al., 2014;Karlstrom et al., 2014;Cook et al., 2016c). Overall, the DON and DOC in supraglacial streams and cryoconite hole water were lower than the DON and DOC in all surface ice habitats and significantly lower than the surface ice with high visible impurities (Figures 4 and 6). Our data, therefore, likely indicate a retention of organic nutrient phases within surface ice environments. One mechanism of possible retention is the production of extracellular polymeric substances (EPS). Algae and bacteria produce EPS which can alter the physical and chemical environment around their cells (Angelaalincy et al., 2017;Stibal et al., 2012a). For example, it has been shown that EPS are used by cyanobacteria in cryoconite holes to bind mineral particles together creating the cryoconite granules at the bottom of the hole (Yallop et al., 2012;Musilova et al., 2016;Stibal et al., 2012b). EPS exists in the colliodal form and when analysed from melted surface ice samples, it is likely constrained in the dissolved organic fraction (Hodson et al., 2010;Pereira et al., 2009). Yet, it is possible that this retention is transitory, and ice surface habitats have the potential to supply a large pulse of dissolved organic nutrients to downstream ecosystems. For example, Musilova et al., 2017 reported that at the margin of the GrIS, DOC remaining in surface ice at the end of the ablation season likely froze over winter and was released the following ablation season through ice melt. The downstream export of DOM from the Dark Zone of the GrIS is currently unknown.

4.4 Stoichiometry of different supraglacial environments

Carbon, nitrogen and phosphorus are required by all cells for balanced growth. The generalised stoichiometry for marine phytoplankton, the Redfield Ratio, is 106:16:1 (Redfield, 1958). It is important to note, however, that while the Redfield Ratio is commonly used as the main stoichiometry reference, it is a specific ratio for marine aquatic environments only. Differing stoichiometries have been reported for diverse environments. For example, Barrett et al., (2017) investigated different environments in the Dry Valleys of Antarctica and found average N:P ratios for surface ice and snow environments and cryoconite holes on glaciers to be 21:1 and 15:1, respectively (Tranter et al., 2004). The average N:P ratios in the same Dry Valley site for streams and lakes fed by glacier melt were 12:1 and 25:1, respectively (Foreman et al., 2004;Lawson et al., 2004). The variability and changes in N:P ratios over time were caused mainly by the presence and activity of microorganisms in the environment and the geochemical availability of nitrogen and phosphorus in the area (Barrett et al., 2007). Furthermore, Lutz et al., 2017 investigated the particulate C:N:P ratios of snow and ice habitats in Sweden and Svalbard. They found high particulate C:N and low particulate N:P ratios, which they concluded as likely N-limitation rather than a more common P-limitation.

Here, we examine the DOC:DON:DOP ratios of melted surface ice samples in an attempt to determine the limiting nutrient of supraglacial environments in the Dark Zone. The dissolved organic C:N:P ratios reported for our surface ice samples are notably higher than the Redfield Ratio, indicating that the system could be P-limited. For example, DON:DOP (49, 78, 116) and DOC:DOP (797, 1166, 2013) ratios reported respectively for low, medium and high surface ice environments are extremely high compared to their 16:1 and 106:1 Redfield ratio counterparts (Table 1).

They also increase as the amount of visible impurities increase. In contrast, DOC:DON ratios are on average only two times higher than the Redfield ratio of 6.6:1 (Table 1). DOC:DOP ratios increase with the amount of visible impurities at a greater rate than DOC:DON ratios for surface ice habitats. This indicates that the more algal biomass present, the higher the retention of DOP, compared to DON (Table 1), suggesting that P-limitation increases with higher algal biomass loading in surface ice habitats.

High DOC:DOP and DON:DOP ratios have been documented in other glacial polar aquatic environments. Stibal et al., (2008) showed that DOC:DOP ratios were ~10 times higher than the Redfield ratio on a Svalbard glacier and that DON:DOP ratios exceed the balanced ratio by a factor of three. This is not entirely surprising as P is a rock-derived mineral that is only released into the dissolved phase by chemical and physical weathering. When compared to alpine glaciers, ice sheet surface environments receive less lithological debris via terrestrial and atmospheric processes, due to their relative proximity to source material. It is, therefore, reasonable for dissolved phosphorus to be the limiting nutrient compared to nitrogen and carbon, both of which are more readily available from the atmosphere.

Cryoconite, a rock derived substance with a high organic carbon content, is found in abundance on many polar ice surfaces and covers 0.5% of the surface ice in the ablation zone of the GrIS (Gribbon, 1979;Bagshaw et al., 2013;Stibal et al., 2012b;Ryan et al., 2018;Cook et al., 2016a). Stibal et al., (2008) investigated the potential bioavailability of phosphorus from cryoconite in cryoconite holes on a Svalbard glacier and found the potentially bioavailable pool of phosphorus in cryoconite to be ~0.16mg g^{-1}. While investigations into the ability of microbes to utilize this particulate inorganic phosphorus pool have yet to be conducted, Tedstone et al., (2017) noted that widespread ice algal blooms may only occur where abundant particulates are available as they could be providing necessary nutrients for the ice algal assemblages. Clearly, further investigation into the influence of particulate phosphorus sources and utilization is needed to fully understand the nutrient cycle occurring in supraglacial environments as the dissolved nutrient input might only represent a portion of the existing cycle.

5. Conclusion

We conclude that ice algal assemblages that bloom in the Dark Zone of the GrIS during the ablation season are the main drivers of the nutrient cycling occurring in melting surface ice environments. Our data indicates a rapid uptake of dissolved inorganic nutrients and a high production of dissolved organic carbon, nitrogen and phosphorus. The relatively high concentrations of dissolved organic nutrients found on the ice surface, combined with reduced secondary production relative to net primary production, suggests an inefficient or inhibited microbial loop for the remineralization of organic nutrient stocks (Yallop et al., 2012). Furthermore, the contrast in dissolved organic nutrient concentrations in surface ice environments compared to supraglacial streams and cryoconite hole water point to retention of nutrients by ice algae. This is due to EPS comprising a portion of the dissolved organic nutrient pool, and its adhesive properties. This retention could result in supraglacial environments acting as large sources of

dissolved organic nutrients for downstream ecosystems, yet the export of DOM from the Dark Zone it is still unknown.

Data Availability

All data will be made available upon acceptance and publication of the article. Data will be inputted into an open access file.

Acknowledgments

The authors would like to thank and acknowledge the entire Black & Bloom team, especially those involved in the sample collection conducted in the 2016 field season.

Team List

Liane G. Benning (GFZ German Research Centre for Geosciences, Potsdam, Germany), James B. McQuaid (University of Leeds, Leeds, UK), Andrew J. Hodson (University Centre in Svalbard, Longyearbyen, Norway & Western Norway University of Applied Sciences, Bergen, Norway), Edward Hanna (University of Lincoln, Lincoln, UK), Tristram D. L. Irvine-Fynn (Aberystwyth University, Aberystwyth, UK), Jonathan L. Bamber (University of Bristol, Bristol, UK), Stefanie Lutz (GFZ German Research Centre for Geosciences, Potsdam, Germany), Miranda J. Nicholes (University of Bristol, Bristol, UK), Marek Stibal (Charles University, Prague, Czech Republic), Jason E. Box (Geological Survey of Denmark and Greenland, Copenhagen, Denmark).

Author contribution

MT, AA and MY conceived and designed the study. AH, CW, MT, AA, AT, JM, JC and the Black & Bloom group collected the samples. CW provided algal counts for the mid to late ablation periods. AH conducted all the nutrient analysis and was aided by FS in the instrument maintenance and data analysis. AH wrote the paper with inputs from MT, CW, AT and AA. All authors reviewed the final manuscript.

Competing Interests

The authors declare they have no conflicts of interest.

Biogeosciences Discuss., https://doi.org/10.5194/bg-2019-69
Manuscript under review for journal Biogeosciences
Discussion started: 4 April 2019

Funding

This project has received funding from the European Union's Horizon 2020 research and innovation programme under the Marie Sklodowska-Curie grant agreement No 675546. This work was also funded in part by the UK Natural Environment Research Council Consortium Grant 'Black and Bloom' (NE/M0212025).

Biogeosciences Discuss., https://doi.org/10.5194/bg-2019-69
Manuscript under review for journal Biogeosciences
Discussion started: 4 April 2019

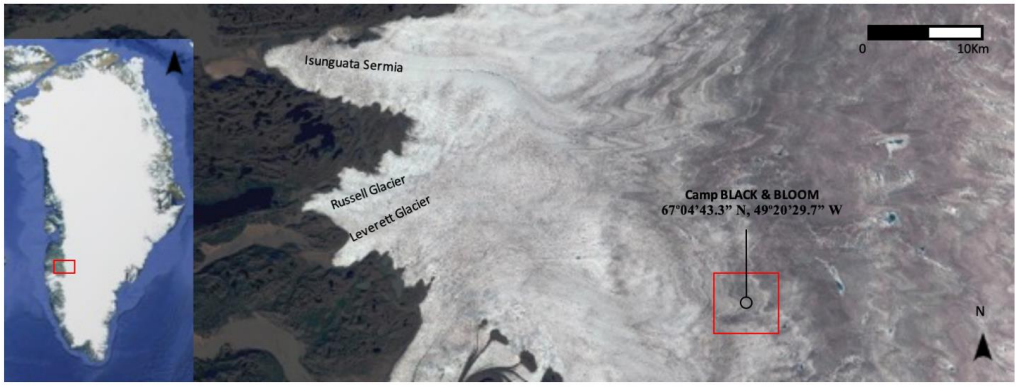

Figure 01. Map showing location of Camp BLACK & BLOOM 2016 (67°04'43.3"N, 49°20'29.7"W). Background image sourced from Sentinel 2, taken on 26/7/2016.

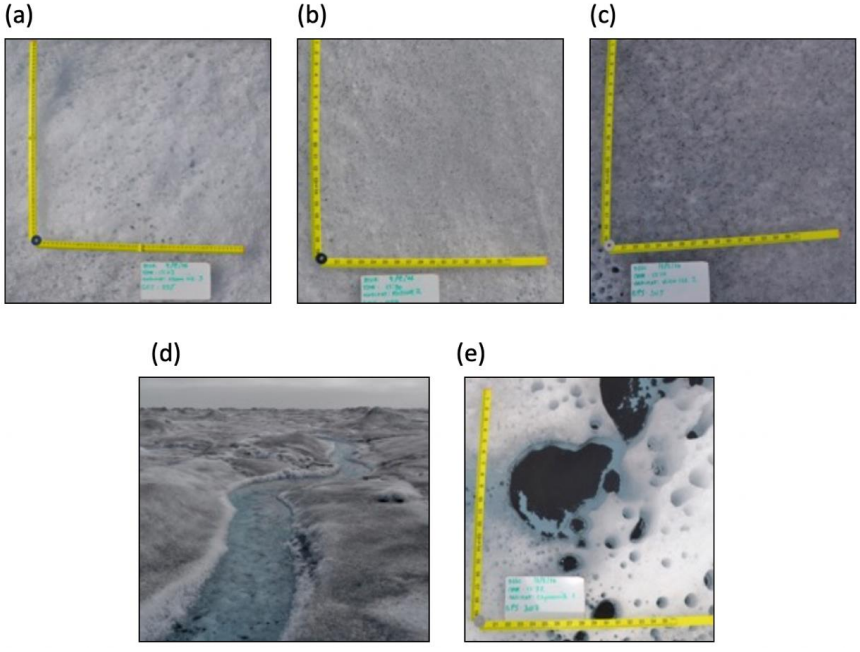

Figure 02: The five supraglacial habitats sampled: **(a)** ice with low visible impurities, **(b)** ice with medium visible impurities, **(c)** ice with high visible impurities, **(d)** supraglacial stream, **(e)** cryoconite hole.

Biogeosciences Discuss., https://doi.org/10.5194/bg-2019-69
Manuscript under review for journal Biogeosciences
Discussion started: 4 April 2019

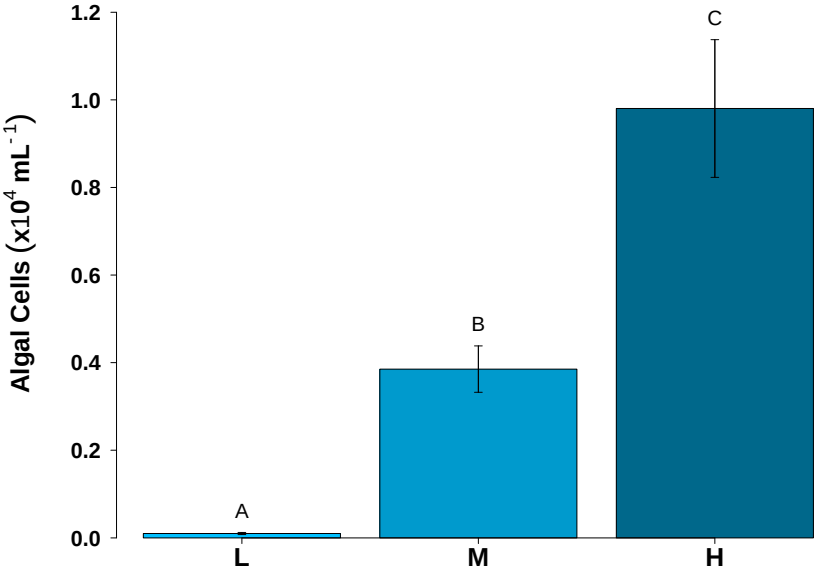

373

374 Figure 03: Algal cell abundance in ice surface ice habitats (mean ± SE, n=19 for each habitat). **L**- ice with low
375 visible impurities, **M**- ice with medium visible impurities and **H**- ice with high visible impurities. *Uppercase*
376 *letters* denote homogeneous subsets derived from post-hoc TukeyHSD analysis on a significant 1-way ANOVA
377 in relation to habitat type.

Biogeosciences Discuss., https://doi.org/10.5194/bg-2019-69
Manuscript under review for journal Biogeosciences
Discussion started: 4 April 2019

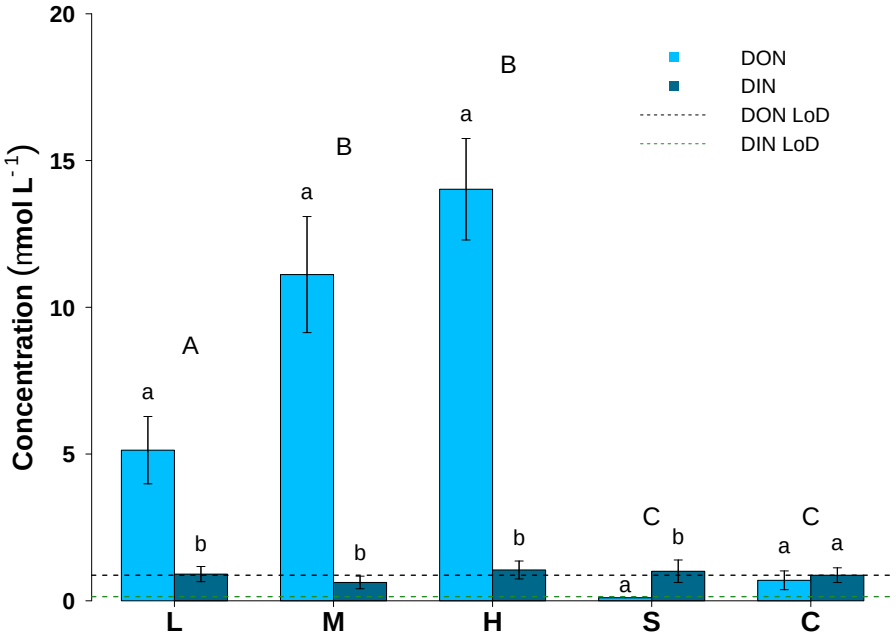

Figure 04: Dissolved Organic Nitrogen (DON) and Dissolved Inorganic Nitrogen (DIN) concentrations for all surface habitats (mean ± SE, n=17 for **L**,**M**,**H**, n=9 for **S** and n=10 for **C**). **L**- ice with low visible impurities, **M**- ice with medium visible impurities, **H**- ice with high visible impurities, **S**- supraglacial stream water and **C**- cryoconite hole water. LOD line depicts the limit of detection of the instrument. *Uppercase letters* denote homogeneous subsets derived from post-hoc TukeyHSD analysis on a significant 1-way ANOVA in relation to dissolved nitrogen phase. *Lowercase letters* denote T-test comparisons in relation to habitat type.

Biogeosciences Discuss., https://doi.org/10.5194/bg-2019-69
Manuscript under review for journal Biogeosciences
Discussion started: 4 April 2019

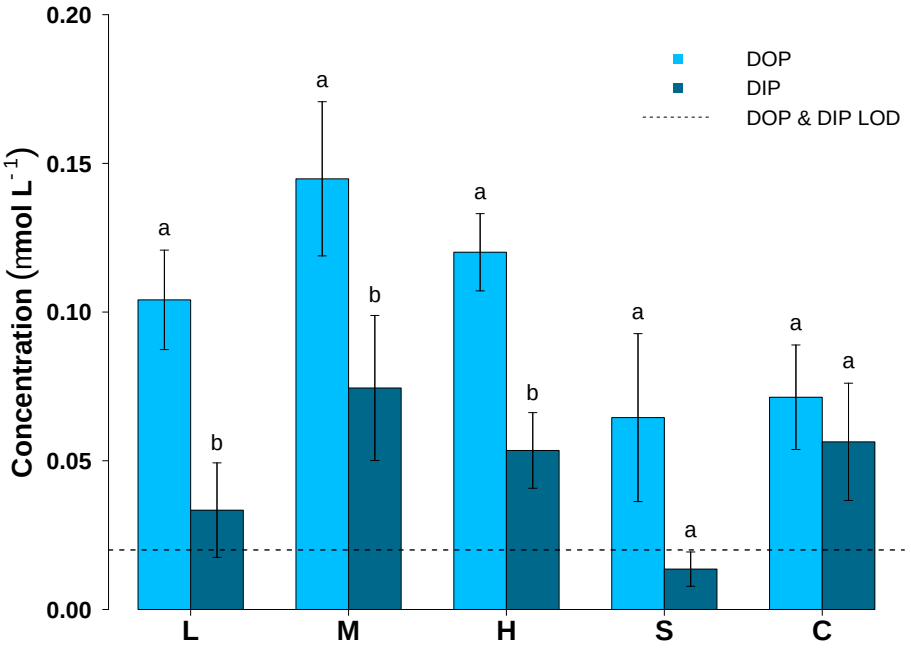

385

386 Figure 05: Dissolved Organic Phosphorus (DOP) and Dissolved Inorganic Phosphorus (DIP) concentrations for
387 all surface ice habitats (mean ± SE, n=17 for **L**,**M**,**H**, n=9 for **S** and n=10 for **C**). **L**- ice with low visible
388 impurities, **M**- ice with medium visible impurities, **H**- ice with high visible impurities, **S**- supraglacial stream
389 water and **C**- cryoconite hole water. LOD line depicts the limit of detection of the instrument. *Lowercase*
390 *letters* denote T-test comparisons in relation to habitat type.

Biogeosciences Discuss., https://doi.org/10.5194/bg-2019-69
Manuscript under review for journal Biogeosciences
Discussion started: 4 April 2019

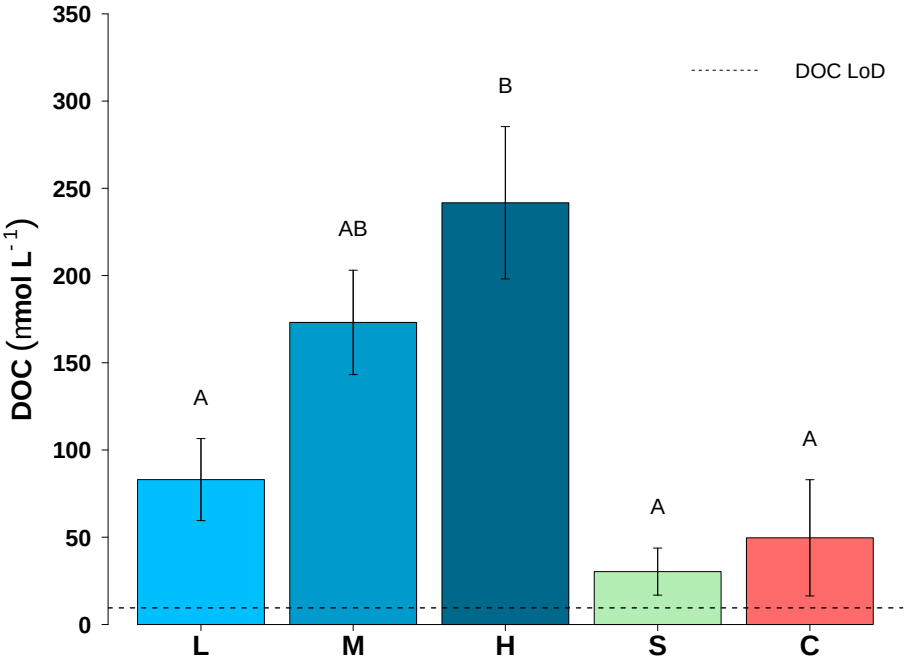

391

392 Figure 06: Dissolved Organic Carbon (DOC) concentrations for all five surface habitats (mean ± SE, n=17 for
393 **L**,**M**,**H**, n=9 for **S** and n=10 for **C**). **L**- ice with low visible impurities, **M**- ice with medium visible impurities,
394 **H**- ice with high visible impurities, **S**- supraglacial stream water and **C**- cryoconite hole water. LOD line
395 depicts the limit of detection of the instrument. *Uppercase letters* denote homogeneous subsets derived from
396 post-hoc TukeyHSD analysis on a significant 1-way ANOVA in relation to habitat type.

Biogeosciences Discuss., https://doi.org/10.5194/bg-2019-69
Manuscript under review for journal Biogeosciences
Discussion started: 4 April 2019

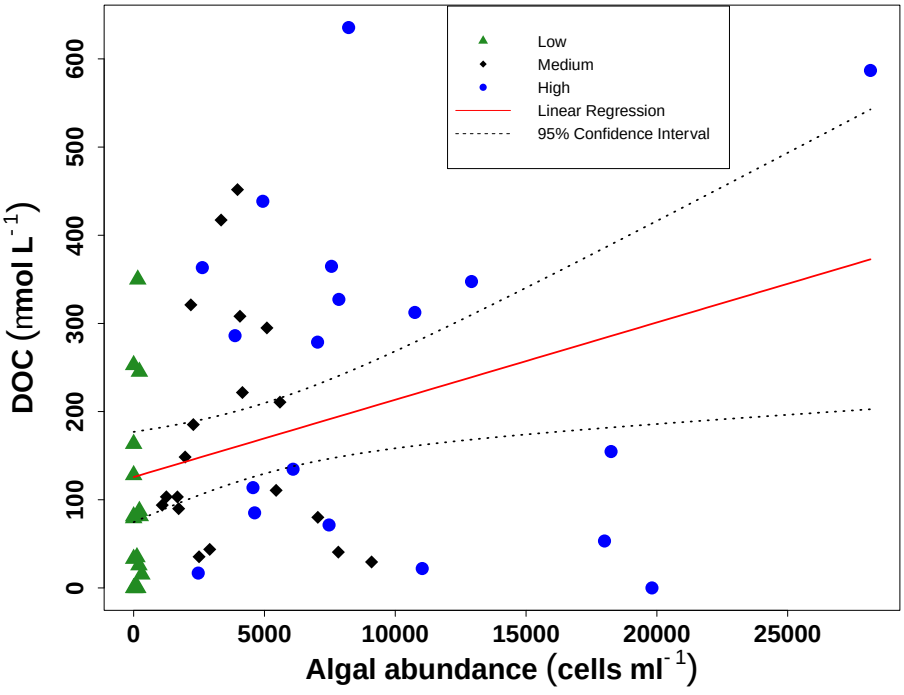

Figure 07: The correlation between DOC concentration and algal cell abundance across ice with low, medium and high visible impurities. R^2=0.1, p<0.01, n=57 for the least squares linear regression.

References

Angelaalincy, M., Senthilkumar, N., Karpagam, R., Kumar, G. G., Ashokkumar, B., and Varalakshmi, P.: Enhanced Extracellular Polysaccharide Production and Self-Sustainable Electricity Generation for PAMFCs by Scenedesmus sp. SB1, ACS Omega, 2, 3754-3765, doi: 10.1021/acsomega.7b00326, 2017.

Bagshaw, E. A., Tranter, M., Fountain, A. G., Welch, K., Basagic, H. J., and Lyons, W. B.: Do Cryoconite Holes have the Potential to be Significant Sources of C, N, and P to Downstream Depauperate Ecosystems of Taylor Valley, Antarctica?, Arctic, Antarctic, and Alpine Research, 45, 440-454, doi: 10.1657/1938-4246-45.4.440, 2013.

Barrett, J. E., Virginia, R. A., Lyons, W. B., McKnight, D. M., Priscu, J. C., Doran, P. T., Fountain, A. G., Wall, D. H., and Moorhead, D. L.: Biogeochemical stoichiometry of Antarctic Dry Valley ecosystems, Journal of Geophysical Research, 112, doi: 10.1029/2005jg000141, 2007.

Box, J., Fettweis, X., Stroeve, J., Tedesco, M., Hall, D., and Steffen, K.: Greenland ice sheet albedo feedback: thermodynamics and atmospheric drivers, The Cryosphere, 6, 821-839, doi: 10.5194/tc-6-821-2012, 2012.

Christner, B. C., Lavender, H. F., Davis, C. L., Oliver, E. E., Neuhaus, S. U., Myers, K. F., Hagedorn, B., Tulaczyk, S. M., Doran, P. T., and Stone, W. C.: Microbial processes in the weathering crust aquifer of a temperate glacier, The Cryosphere, 12, 3653-3669, doi: 10.5194/tc-12-3653-2018, 2018.

Cook, J., Edwards, A., Takeuchi, N., and Irvine-Fynn, T.: Cryoconite: the dark biological secret of the cryosphere, Progress in Physical Geography, 40, 66-111, doi: 10.1177/0309133315616574, 2016a.

Cook, J., Hodson, A. J., Taggart, A., Mernild, S. H., and Tranter, M.: A predictive model for the spectral "bioalbedo" of snow, Journal of Geophysical Research: Earth Surface, 122, 434-454, doi: 10.1002/2016JF003932, 2017a.

Cook, J. M., Edwards, A., Bulling, M., Mur, L. A., Cook, S., Gokul, J. K., Cameron, K. A., Sweet, M., and Irvine-Fynn, T. D.: Metabolome-mediated biocryomorphic evolution promotes carbon fixation in Greenlandic cryoconite holes, Environmental Microbiology, 18, 4674-4686, doi: 10.1111/1462-2920.13349, 2016b.

Cook, J. M., Hodson, A. J., and Irvine-Fynn, T. D.: Supraglacial weathering crust dynamics inferred from cryoconite hole hydrology, Hydrological Processes, 30, 433-446, doi: 10.1002/hyp.10602, 2016c.

Dodds, W. K.: What controls levels of dissolved phosphate and ammonium in surface waters?, Aquatic Sciences, 55, 132-142, doi: 1015-1621/93/020132-11, 1993.

Enderlin, E. M., Howat, I. M., Jeong, S., Noh, M. J., Van Angelen, J. H., and Van Den Broeke, M. R.: An improved mass budget for the Greenland ice sheet, Geophysical Research Letters, 41, 866-872, doi: 10.1002/2013GL059010, 2014.

Foreman, C. M., Wolf, C. F., and Priscu, J. C.: Impact of episodic warming events, Aquatic Geochemistry, 10, 239-268, 2004.

Gardner, A. S., and Sharp, M. J.: A review of snow and ice albedo and the development of a new physically based broadband albedo parameterization, Journal of Geophysical Research: Earth Surface, 115, doi: 10.1029/2009JF001444, 2010.

Grasshoff, K., Kremling, K., and Ehrhardt, M.: Methods of seawater analysis, John Wiley & Sons, 1999.

Gribbon, P.: Cryoconite holes on Sermikavsak, west Greenland, Journal of Glaciology, 22, 177-181, 1979.

Hawkings, J., Wadham, J., Tranter, M., Telling, J., Bagshaw, E., Beaton, A., Simmons, S.-L., Chandler, D., Tedstone, A., and Nienow, P.: The Greenland Ice Sheet as a hot spot of phosphorus weathering and export in the Arctic, Global Biogeochemical Cycles, 30, 191-210, 10.1002/2015gb005237, 2016.

Hodson, A., Cameron, K., Bøggild, C., Irvine-Fynn, T., Langford, H., Pearce, D., and Banwart, S.: The structure, biological activity and biogeochemistry of cryoconite aggregates upon an Arctic valley glacier: Longyearbreen, Svalbard, Journal of Glaciology, 56, 349-362, 2010.

Hoffman, M. J., Fountain, A. G., and Liston, G. E.: Near-surface internal melting: a substantial mass loss on Antarctic Dry Valley glaciers, Journal of Glaciology, 60, 361-374, doi: 10.3189/2014JoG13J095, 2014.

Irvine-Fynn, T., Edwards, A., Newton, S., Langford, H., Rassner, S., Telling, J., Anesio, A., and Hodson, A.: Microbial cell budgets of an A rctic glacier surface quantified using flow cytometry, Environmental Microbiology, 14, 2998-3012, doi: 10.1111/j.1462-2920.2012.02876.x, 2012.

Johannes, R., and Webb, K. L.: Release of dissolved organic compounds by marine and fresh water invertebrates, Symposium on organic matter in natural waters, 1970, 257,

Karlstrom, L., Zok, A., and Manga, M.: Near-surface permeability in a supraglacial drainage basin on the Llewellyn Glacier, Juneau Icefield, British Columbia, The Cryosphere, 8, 537-546, doi: 10.5194/tc-8-537-2014, 2014.

Kohshima, S., Seko, K., and Yoshimura, Y.: Biotic Acceleration of Glacier Melting in Yala Glacier, Langtang Region, Nepal Himalaya, Snow and Glacier Hydrology, 1993.

Kuhn, M.: The nutrient cycle through snow and ice, a review, Aquatic Sciences, 63, 150-167, doi: 1015-1621/01/020150-18, 2001.

LaChapelle, E.: Errors in ablation measurements from settlement and sub-surface melting, Journal of Glaciology, 3, 458-467, 1959.
Lampert, W.: Release of dissolved organic carbon by grazing zooplankton, Limnology and Oceanography, 23, 831-834, 1978.
Lawson, J., Doran, P. T., Kenig, F., and Priscu, J. C.: Stable carbon and nitrogen isotopic, Aquatic Geochemistry, 10, 269-301, 2004.
Lutz, S., Anesio, A. M., Edwards, A., and Benning, L. G.: Linking microbial diversity and functionality of arctic glacial surface habitats, Environ Microbiol, 19, 551-565, doi: 10.1111/1462-2920.13494, 2017.
Maccario, L., Sanguino, L., Vogel, T. M., and Larose, C.: Snow and ice ecosystems: not so extreme, Res Microbiol, 166, 782-795, doi: 10.1016/j.resmic.2015.09.002, 2015.
Müller, F., and Keeler, C. M.: Errors in short-term ablation measurements on melting ice surfaces, Journal of Glaciology, 8, 91-105, 1969.
Munro, D. S.: Comparison of melt energy computations and ablatometer measurements on melting ice and snow, Arctic Alpine Research, 22, 153-162, doi: 10.1080/00040851.1990.12002777, 1990.
Musilova, M., Tranter, M., Bamber, J. L., Takeuchi, N., and Anesio, A.: Experimental evidence that microbial activity lowers the albedo of glaciers, Geochemical Perspectives Letters, 106-116, doi: 10.7185/geochemlet.1611, 2016.
Musilova, M., Tranter, M., Wadham, J., Telling, J., Tedstone, A., and Anesio, Alexandre M.: Microbially driven export of labile organic carbon from the Greenland ice sheet, Nature Geoscience, 10, 360-365, doi: 10.1038/ngeo2920, 2017.
Nicholes, M. J., Williamson, C. J., Tranter, M., Holland, A. T., Poniecka, E., Yallop, M. L., The Black and Bloom Team, And Anesio, A. M.: Bacterial dynamics in supraglacial habitats of the Greenland Ice Sheet, Front Microbiol, in review.
Pereira, S., Zille, A., Micheletti, E., Moradas-Ferreira, P., De Philippis, R., and Tamagnini, P.: Complexity of cyanobacterial exopolysaccharides: composition, structures, inducing factors and putative genes involved in their biosynthesis and assembly, FEMS Microbiol Rev, 33, 917-941, doi: 10.1111/j.1574-6976.2009.00183.x, 2009.
Rassner, S. M., Anesio, A. M., Girdwood, S. E., Hell, K., Gokul, J. K., Whitworth, D. E., and Edwards, A.: Can the bacterial community of a high Arctic glacier surface escape viral control?, Front Microbiol, 7, 956, doi: 10.3389/fmicb.2016.00956, 2016.
Redfield, A., Ketchum, B., and Richards, F.: The influence of organisms on the composition of sea water., Hill MH (ed) The sea, Intersci. Publ., Wiley, New York, 554 pp., 1963.
Redfield, A. C.: The biological control of chemical factors in the environment, American Scientist, 46, 230A-221, 1958.
Remias, D., Schwaiger, S., Aigner, S., Leya, T., Stuppner, H., and Lütz, C.: Characterization of an UV-and VIS-absorbing, purpurogallin-derived secondary pigment new to algae and highly abundant in M esotaenium berggrenii (Z ygnematophyceae, Chlorophyta), an extremophyte living on glaciers, FEMS Microbiol Ecol, 79, 638-648, doi: 10.1111/j.1574-6941.2011.01245.x, 2012.
Rignot, E., and Kanagaratnam, P.: Changes in the velocity structure of the Greenland Ice Sheet, Science, 311, 986-990, doi: 10.1126/science.1121381, 2006.
Rignot, E., Velicogna, I., van den Broeke, M. R., Monaghan, A., and Lenaerts, J. T.: Acceleration of the contribution of the Greenland and Antarctic ice sheets to sea level rise, Geophysical Research Letters, 38, doi: 10.1029/2011GL046583, 2011.
Ryan, J. C., Hubbard, A., Stibal, M., Irvine-Fynn, T. D., Cook, J., Smith, L. C., Cameron, K., and Box, J.: Dark zone of the Greenland Ice Sheet controlled by distributed biologically-active impurities, Nature Communications 9, 1065, doi: 10.1038/s41467-018-03353-2, 2018.
Sasgen, I., van den Broeke, M., Bamber, J. L., Rignot, E., Sørensen, L. S., Wouters, B., Martinec, Z., Velicogna, I., and Simonsen, S. B.: Timing and origin of recent regional ice-mass loss in Greenland, Earth Planetary Science Letters, 333, 293-303, doi: 10.1016/j.epsl.2012.03.033, 2012.
Shepherd, A., Ivins, E. R., Geruo, A., Barletta, V. R., Bentley, M. J., Bettadpur, S., Briggs, K. H., Bromwich, D. H., Forsberg, R., and Galin, N.: A reconciled estimate of ice-sheet mass balance, Science, 338, 1183-1189, doi: 10.1126/science.1228102, 2012.
Shimada, R., Takeuchi, N., and Aoki, T.: Inter-annual and geographical variations in the extent of bare ice and dark ice on the Greenland Ice Sheet derived from MODIS satellite images, Frontiers in Earth Science, 4, 43, doi: 10.3389/feart.2016.00043, 2016.
Shrivastava, A., and Gupta, V. B.: Methods for the determination of limit of detection and limit of quantitation of the analytical methods, Chronicles of Young Scientists, 2, 21, doi: 10.4103/2229-5186.79345, 2011.
Solorzano, L.: Determination of Ammonia in Natural Waters by the Phenolhypochlorite Method, Limnology and Oceanography, 14, 799-801, 1969.

Stibal, M., Tranter, M., Benning, L. G., and Rehak, J.: Microbial primary production on an Arctic glacier is insignificant in comparison with allochthonous organic carbon input, Environ Microbiol, 10, 2172-2178, doi: 10.1111/j.1462-2920.2008.01620.x, 2008a.

Stibal, M., Tranter, M., Telling, J., and Benning, L. G.: Speciation, phase association and potential bioavailability of phosphorus on a Svalbard glacier, Biogeochemistry, 90, 1-13, doi: 10.1007/s, 2008b.

Stibal, M., Anesio, A. M., D., B. C. J., and Tranter, M.: Phosphatase activity and organic phosphorus turnover on a high Arctic glacier, Biogeosciences, 6, 913-922, 2009.

Stibal, M., Šabacká, M., and Žárský, J.: Biological processes on glacier and ice sheet surfaces, Nature Geoscience, 5, 771-774, 10.1038/ngeo1611, 2012a.

Stibal, M., Telling, J., Cook, J., Mak, K. M., Hodson, A., and Anesio, A. M.: Environmental controls on microbial abundance and activity on the greenland ice sheet: a multivariate analysis approach, Microb Ecol, 63, 74-84, doi: 10.1007/s00248-011-9935-3, 2012b.

Stibal, M., Box, J. E., Cameron, K. A., Langen, P. L., Yallop, M. L., Mottram, R. H., Khan, A. L., Molotch, N. P., Chrismas, N. A., and Calì Quaglia, F.: Algae drive enhanced darkening of bare ice on the Greenland ice sheet, Geophysical Research Letters, 44, doi: 10.1002/2017GL075958, 2017a.

Stroeve, J., Box, J. E., Wang, Z., Schaaf, C., and Barrett, A.: Re-evaluation of MODIS MCD43 Greenland albedo accuracy and trends, Remote sensing of environment, 138, 199-214, doi: 10.1016/j.rse.2013.07.023, 2013.

Tedstone, A. J., Bamber, J. L., Cook, J. M., Williamson, C. J., Fettweis, X., Hodson, A. J., and Tranter, M.: Dark ice dynamics of the south-west Greenland Ice Sheet, The Cryosphere, 11, 2491-2506, doi: 10.5194/tc-11-2491-2017, 2017.

Telling, J., Anesio, A. M., Tranter, M., Irvine-Fynn, T., Hodson, A., Butler, C., and Wadham, J.: Nitrogen fixation on Arctic glaciers, Svalbard, Journal of Geophysical Research, 116, doi: 10.1029/2010jg001632, 2011.

Telling, J., Stibal, M., Anesio, A. M., Tranter, M., Nias, I., Cook, J., Bellas, C., Lis, G., Wadham, J. L., Sole, A., Nienow, P., and Hodson, A.: Microbial nitrogen cycling on the Greenland Ice Sheet, Biogeosciences, 9, 2431-2442, doi: 10.5194/bg-9-2431-2012, 2012.

Telling, J., Anesio, A. M., Tranter, M., Fountain, A. G., Nylen, T., Hawkings, J., Singh, V. B., Kaur, P., Musilova, M., and Wadham, J. L.: Spring thaw ionic pulses boost nutrient availability and microbial growth in entombed Antarctic Dry Valley cryoconite holes, Front Microbiol, 5, 694, doi: 10.3389/fmicb.2014.00694, 2014.

Tranter, M., Fountain, A. G., Fritsen, C. H., Berry Lyons, W., Priscu, J. C., Statham, P. J., and Welch, K. A.: Extreme hydrochemical conditions in natural microcosms entombed within Antarctic ice, Hydrological Processes, 18, 379-387, doi: 10.1002/hyp.5217, 2004.

Warren, S. G., and Wiscombe, W. J.: A model for the spectral albedo of snow. II: Snow containing atmospheric aerosols, Journal of the Atmospheric Sciences, 37, 2734-2745, 1980.

Warren, S. G.: Impurities in snow: Effects on albedo and snowmelt, Annals of Glaciology, 5, 177-179, 1984.

Warren, S. G., and Wiscombe, W. J.: Dirty snow after nuclear war, Nature, 313, 467, 1985.

Wientjes, I. G. M., and Oerlemans, J.: An explanation for the dark region in the western melt zone of the Greenland ice sheet, The Cryosphere, 4, 261-268, doi: 10.5194/tc-4-261-2010, 2010.

Wientjes, I. G. M., Van De Wal, R. S. W., Schwikowski, M., Zapf, A., Fahrni, S., and Wacker, L.: Carbonaceous particles reveal that Late Holocene dust causes the dark region in the western ablation zone of the Greenland ice sheet, Journal of Glaciology, 58, 787-794, doi: 10.3189/2012JoG11J165, 2012.

Williamson, C. J., Anesio, A. M., Cook, J., Tedstone, A., Poniecka, E., Holland, A., Fagan, D., Tranter, M., and Yallop, M. L.: Ice algal bloom development on the surface of the Greenland Ice Sheet, FEMS Microbiol Ecol, 94, doi: 10.1093/femsec/fiy025, 2018.

Yallop, M. L., Anesio, A. M., Perkins, R. G., Cook, J., Telling, J., Fagan, D., MacFarlane, J., Stibal, M., Barker, G., Bellas, C., Hodson, A., Tranter, M., Wadham, J., and Roberts, N. W.: Photophysiology and albedo-changing potential of the ice algal community on the surface of the Greenland ice sheet, ISME J, 6, 2302-2313, doi: 10.1038/ismej.2012.107, 2012.

Biogeosciences Discuss., https://doi.org/10.5194/bg-2019-69
Manuscript under review for journal Biogeosciences
Discussion started: 4 April 2019

578 Table 01: Nutrient concentrations for the five supraglacial habitats. For each nutrient, the mean ± SD is
579 provided, followed by the range of values. Concentrations are expressed in µmol; nutrient ratios are in
580 µmol/µmol.

	Ice Habitat			Supraglacial Stream	Cryoconite Hole	Field Blank
	Low	**Medium**	**High**			
NH_4^+	0.97±1.1 0-4.0	0.91±1.3 0-3.6	1.4±1.7 0-5.5	1.1±1.5 0-4.0	0.88±1.1 0-3.0	1.1±1.4 0-3.3
NO_2^-	0.00±0.00 0	0.00±0.00 0	0.00±0.00 0	0.00±0.00 0	0.00±0.00 0	0.00±0.01 0
NO_3^-	0.00±0.00 0	0.00±0.00 0	0.00±0.00 0	0.00±0.00 0	0.22±0.71 0-2.2	0.00±0.00 0
DON	4.5±3.3 0-10	17±10 0-40	15±7.4 3.2-27	0.09±0.27 0-0.82	0.50±1.0 0-3.2	0±0 0
DIP	0.01±0.02 0-0.09	0.01±0.03 0-0.14	0.00±0.02 0-0.06	0.00±0.00 0	0.00±0.00 0	0±0 0
DOP	0.04±0.09 0-0.27	0.17±0.15 0-0.48	0.07±0.11 0-0.25	0.00±0.00 0	0.02±0.07 0-0.21	0.00±0.00 0
DOC	86±107 0-349	183±135 29-451	245±200 0-636	30±40 0-84	10±18 0-49	12±17 0-35
DON:DOP	49.3	78.9	116.8	0.00	9.4	Na
DOC:DOP	797.8	1166.2	2013.3	455.3	671.3	Na
DOC:DON	16.2	15.6	17.2	Na	71.3	Na
DIN:DIP	27.2	8.4	19.6	74.1	15.5	Na
Sample Size (n)	17	17	17	9	10	7

581

582

583 DON Dissolved Organic Nitrogen

584 DIP Dissolved Inorganic Phosphorus

585 DOP Dissolved Organic Phosphorus

586 DOC Dissolved Organic Carbon

587